Advances in Nano Research, *Vol. 6 No. 1* (*2018*) *39-55*
DOI: https://doi.org/10.12989/anr.2018.6.1.039

Forced vibration analysis of cracked functionally graded microbeams

Şeref D. Akbaş *

Department of Civil Engineering, *Bursa Technical University*, *Yıldırım Campus*, *Yıldırım*, *Bursa 16330*, *Turkey*

(*Received December 11, 2017, Revised January 22, 2018, Accepted April 3, 2018*)

Abstract. Forced vibration analysis of a cracked functionally graded microbeam is investigated by using modified couple stress theory with damping effect. Mechanical properties of the functionally graded beam change vary along the thickness direction. The crack is modelled with a rotational spring. The Kelvin-Voigt model is considered in the damping effect. In solution of the dynamic problem, finite element method is used within Timoshenko beam theory in the time domain. Influences of the geometry and material parameters on forced vibration responses of cracked functionally graded microbeams are presented.

Keywords: functionally graded materials; microbeam; modified couple stress theory; forced vibration analysis; crack

1. Introduction

With the development of technology, micro structures are used in many applications (sensor, microscale electromechanical systems). The classical mechanical theories fail to satisfy in the solution of the micro elements because it is not effort the size-effect in the micro-scale. So, the nonlocal theories (couple stress and gradient theories) must be used in the mechanics of the micro structures which effort the size-effect. Functionally graded materials (FGMs) are a type of composite which consist different phases of material, where the properties of materials change in a direction. FGMs have a lot of applications such as, aircrafts, biomedical products, space vehicles. With the development of technology, functionally graded materials are used in micro structural structures for example, electrically actuated micro electromechanical devices , atomic force microscopes (Witvrouw and Mehta 2005, Fu *et al*. 2003, Hasanyan *et al*. 2008, Zhang and Fu 2012, Lü *et al*. 2009).

The nonlocal theory proposed by Eringen (1972) that analyze nano/micro structures. Many researcher have used and developed the nonlocal theory in the analysis nano/micro structures (Toupin 1962, Lam *et al*. 2003, Mindlin 1963). Yang *et al*. (2002) presented expressions of strain energy with a scale factor in the Modified Couple Stress Theory (MCST). Nonlocal theories broadly utilized for mechanical analysis of FGM nano/micro and homogeneous beams (Park and Gao 2006, Ansari *et al*. 2011, Wang *et al*. 2012, Asghari *et al*. 2010, Liu and Reddy 2011, Salamat-Talab *et al*. 2012, Kocatürk and Akbaş 2013a, b, Şimşek and Reddy 2013, Belabed *et al*. 2014,

*Corresponding author, Associate Professor, E-mail: serefda@yahoo.com

http://www.techno-press.org/?journal=anr&subpage=5 ISSN: 2287-237X (Print), 2287-2388 (Online)

Mahi *et al*. 2015, Hamidi *et al*. 2015, Tagrara *et al*. 2015, Şimşek *et al*. 2013, Ansari *et al*. 2014, Zamanzadeh *et al*. 2014, Akgöz and Civalek 2013, 2014, Akbaş and Kocatürk 2013, Ke *et al*. 2012, Sedighi 2014, Sedighi *et al*. 2014, Al-Basyouni *et al*. 2015, Chaht *et al*. 2015, Belkorissat *et al*. 2015, Aissani *et al*. 2015, Hadji *et al*. 2016, Akbaş 2013, 2015a, b, 2016a, b, 2017a, b, 2017c, d, e, f, 2018, Hadji 2017 , Zouatnia *et al*. 2017, Ebrahimi and Salari 2015, Ebrahimi and Barati 2016a, b, Ebrahimi *et al*. 2017, Nejad and Hadi 2016a, b, Shafiei *et al*. 2016, Bousahla *et al*. 2014, Hebali *et al*. 2014, Meziane *et al*. 2014, Yahia *et al*. 2015, Bourada *et al*. 2015, Bounouara *et al*. 2016, Bennoun *et al*. 2016, Houari *et al*. 2016, Boukhari *et al*. 2016, Abdelaziz *et al*. 2017, Bouafia *et al*. 2017, Khetir *et al*. 2017, Bellifa *et al*. 2017, Besseghier *et al*. 2017, Mouffoki *et al*. 2017, Karami *et al*. 2017, Ahouel *et al*. 2016, Demir and Civalek 2017, Attia 2017). During the processing in the fabrication of micro structures, it can occur crack in the structure's material due to technically problems. In instance, cracks can occur in the thermal fabrication process of the ZnO micro-rods (Fang *et al*. 2003, Fang and Chang 2003). Cracks cause a local flexibility in the cracked structures and structures can lose their structural strength. In the literature, the studies of the cracked micro/nano structures are as follows; Loya *et al*. (2009), Hasheminejad *et al*. (2011), Torabi and Nafar Dastgerdi (2012), Liu *et al*. (2013), Roostai and Haghpanahi (2014), Aissani *et al*. (2015), Yaylı and Çerçevik (2015), Tadi Beni *et al*. (2015), Wang and Wang (2015), Akbaş (2016a, b), Stamenković *et al*. (2016) and Peng *et al*. (2015) analyzed dynamics of cracked nano/micro beams with the nonlocal theories.

In the open literature, forced vibration of cracked FGM microbeams has not been broadly studied. The main aim of presented paper is to fill this absence for cracked FGM microbeams. The work deals with forced vibration responses of cracked FGM a microbeam by using Timoshenko beam theory with MCST. In the solution of the dynamic problem, finite element and Newmark methods are used in the time domain with the damping effect. The influences of crack, geometry and distributions on forced vibration responses of cracked microbeams are examined and discussed.

2. Theory and formulation

A cantilever functionally graded cracked microbeam under a external dynamic load $P(t)$ at the free end is displayed in Fig. 1 according to X, Y, Z coordinate system. L is length, b is width, h is thickness, a indicates the crack depth and L_1 indicates the crack location from the left end in Fig. 1.

The mechanical properties of the microbeam vary along the Y direction based on an exponential distribution

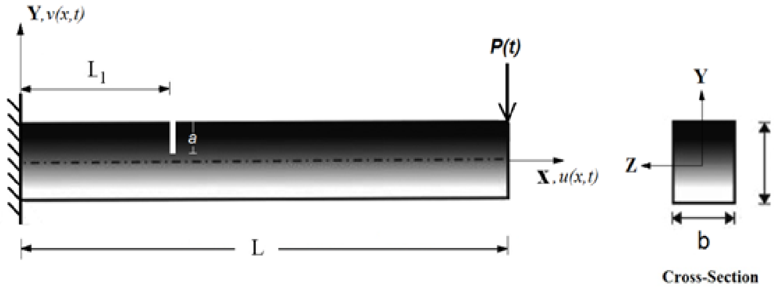

Fig. 1 A cantilever FGM cracked microbeam under a external dynamic point load $P(t)$

$$E(Y) = E_0 e^{\beta Y}, \quad \rho(Y) = \rho_0 e^{\beta Y} \tag{1}$$

In Eq. (1), ρ_0 and E_0 indicate mass density and Young's modulus at $Y = 0$, respectively. β is material distribution parameter which defines the material distribution through *Y* direction. The microbeam becomes a fully top surface material as $\beta = 0$.

In the MCST, the influences of the deviatoric stretch gradient and the dilatation gradient are ignored, so a single material length scale parameter is required, which relates the couple stress to the symmetric part of the rotational gradient. For MCST, the strain energy (*U*) is defined as (Yang *et al*. 2002)

$$U = \int_V (\boldsymbol{\sigma};\boldsymbol{\varepsilon} + \boldsymbol{m};\boldsymbol{\chi})\, dV \tag{2}$$

where $\boldsymbol{\sigma}$, $\boldsymbol{m}$, $\boldsymbol{\chi}$, $\boldsymbol{\varepsilon}$, and are stress, couple stress, curvature and strain tensors respectively, and their details are expressed as follows

$$\boldsymbol{\sigma} = \frac{E(Y)\ \nu(Y)}{(1+\nu(Y))(1-2\nu(Y))}\ tr(\boldsymbol{\varepsilon})I + 2\frac{E(Y)}{2(1+\nu)}\boldsymbol{\varepsilon} \tag{3a}$$

$$\boldsymbol{\varepsilon} = \frac{1}{2}[\nabla\boldsymbol{u} + (\nabla\boldsymbol{u})^T] \tag{3b}$$

$$\boldsymbol{m} = l^2 \frac{E(Y)}{(1+\nu(Y))}\ \boldsymbol{\chi} \tag{3c}$$

$$\boldsymbol{\chi} = \frac{1}{2}[\nabla\boldsymbol{\theta} + (\nabla\boldsymbol{\theta})^T] \tag{3d}$$

where *l* indicates length scale parameter that characterize the couple stress influences. $\boldsymbol{\nu}$ is the Poisson's ratio. $\boldsymbol{\theta}$ and $\boldsymbol{u}$ and indicate rotation and displacement vectors respectively, expressed as follows

$$\boldsymbol{\theta} = \frac{1}{2}\mathrm{curl}\,\boldsymbol{u} \tag{4}$$

Strain and curvature tensor expressions are given in any time *t* according to Timoshenko beam theory as follows

$$\varepsilon_{xx} = \frac{\partial u}{\partial X} = \frac{\partial u(X,t)}{\partial X} - Y\frac{\partial \emptyset(x,t)}{\partial X} \tag{5a}$$

$$\gamma_{xy} = \frac{\partial v}{\partial \mathrm{x}} - \emptyset(x,t) \tag{5b}$$

$$\chi_{xz} = \frac{1}{4}\left(\frac{\partial^2 v(X,t)}{\partial X^2} + \frac{\partial \emptyset(X,t)}{\partial X}\right), \quad \chi_{xx} = \chi_{xy} = \chi_{yy} = \chi_{yz} = \chi_{zz} = 0 \tag{5c}$$

where u and v are horizontal and vertical deflections, respectively. $\emptyset$ indicates the rotation. Constitutive relation of the problem is given with using the Kelvin–Voigt viscoelastic model as follows

$$\sigma_{xx} = E(Y)\left(\left(\frac{\partial \mathrm{u}(X,t)}{\partial X} - Y\frac{\partial \emptyset(x,t)}{\partial X}\right) + \eta_1(\mathrm{Y})\frac{\partial}{\partial t}\left(\frac{\partial \mathrm{u}(X,t)}{\partial X} - Y\frac{\partial \emptyset(x,t)}{\partial X}\right)\right) \tag{6a}$$

$$\sigma_{xy} = k_s\,\frac{E(Y)}{2(1+\nu)}\left(\left(\frac{\partial v}{\partial \mathrm{x}} - \emptyset(x,t)\right) + \eta_2(\mathrm{Y})\frac{\partial}{\partial t}\left(\frac{\partial v}{\partial \mathrm{x}} - \emptyset(x,t)\right)\right) \tag{6b}$$

$$m_{xz} = \frac{1}{2}l^2\,\frac{E(Y)}{2(1+\nu)}\left(\left(\frac{\partial^2 v(X,t)}{\partial X^2} + \frac{\partial \emptyset(X,t)}{\partial X}\right) + \eta_3(\mathrm{Y})\frac{\partial}{\partial t}\left(\frac{\partial^2 v(X,t)}{\partial X^2} + \frac{\partial \emptyset(X,t)}{\partial X}\right)\right) \tag{6c}$$

$$m_{xx} = m_{xy} = m_{yy} = m_{yz} = m_{zz} = 0 \tag{6d}$$

where k_s indicates the shear correction factor, η_1, η_2 and η_3 are the damping ratios in bending, shearing and couple stress, respectively, as follows

$$\eta_1 = \frac{c(Y)}{E(Y)},\quad \eta_2 = \frac{c(Y)\,2(1+\nu(Y))}{E(Y)},\quad \eta_3 = \frac{c(Y)\ (1+\nu(Y))}{2l^2E(Y)} \tag{7}$$

where c indicates the damping coefficient. Substituting Eqs. (5) and (6) into Eq. (2), strain energy is presented as follows

$$\begin{aligned} U_i = \frac{1}{2}\int_0^L \Bigg[& A_{11}\left(\frac{\partial u(X,t)}{\partial X}\right)^2 - 2B_{11}\left(\frac{\partial \mathrm{u}(X,t)}{\partial X}\right)\left(\frac{\partial \emptyset(x,t)}{\partial X}\right) + D_{11}\left(\frac{\partial \emptyset(x,t)}{\partial X}\right)^2 \\ & + k_sA_{55}\left(\frac{\partial v}{\partial \mathrm{x}} - \emptyset(x,t)\right) + \frac{1}{8}l^2A_{55}\left(\frac{\partial^2 v(X,t)}{\partial X^2} + \frac{\partial \emptyset(X,t)}{\partial X}\right)^2\Bigg]dX \end{aligned} \tag{8}$$

where

$$(A_{11}, B_{11}, D_{11}) = \int_A E(Y)(1, Y, Y^2)dA, \qquad A_{55} = \int_A \mu(Y)dA \tag{9}$$

The kinetic energy of the problem (T) is

$$T = \frac{1}{2}\int_0^L \left[I_1\left(\frac{\partial u_0}{\partial t}\right)^2 - 2I_2\left(\frac{\partial u_0}{\partial t}\right)\left(\frac{\partial \emptyset}{\partial t}\right) + I_1\left(\frac{\partial v_0}{\partial t}\right)^2 + I_3\left(\frac{\partial \emptyset}{\partial t}\right)^2\right]dX \tag{10}$$

where

$$(I_1, I_2, I_3) = \int_A \rho(Y)(1, Y, Y^2)dA \tag{11}$$

where ρ indicates the mass density. The dissipation function of the problem (R) is given as follows

$$R=\frac{1}{2}\int_0^L\left(C_1\left(\frac{\partial}{\partial X}\left(\frac{\partial u}{\partial t}\right)\right)^2-2C_2\left(\frac{\partial}{\partial X}\left(\frac{\partial u}{\partial t}\right)\right)\left(\frac{\partial}{\partial X}\left(\frac{\partial \emptyset}{\partial t}\right)\right)+C_3\left(\frac{\partial}{\partial X}\left(\frac{\partial u}{\partial t}\right)\right)^2\right.$$
$$\left.+C_4\left(\frac{\partial}{\partial X}\left(\frac{\partial v}{\partial t}\right)-\left(\frac{\partial \emptyset}{\partial t}\right)\right)^2+\frac{1}{8}l^2C_4\left(\frac{\partial^2}{\partial X^2}\left(\frac{\partial v}{\partial t}\right)+\frac{\partial}{\partial X}\left(\frac{\partial \emptyset}{\partial t}\right)\right)^2\right)dx \tag{12}$$

where

$$(C_1,C_2,C_3)=\int_A E(Y)\eta_1(Y)(1,Y,Y^2)dA,\qquad (C_4)=\int_A \mu\,(Y)\eta_2(Y)dA \tag{13}$$

The potential energy of the external loads (U_e) is given as follows

$$U_e=-\int_0^L[P(x,t)\,v(x,t)]\,dX \tag{14}$$

The Lagrangian functional is given as follows

$$I=T-(U_\mathrm{i}+U_\mathrm{e}) \tag{15}$$

In the finite element solution, two-node beam element with three freedom degrees is used as shown in Fig. 2.

The displacement vector in terms of node displacements and rotation are expressed as

$$\{q(t)\}_\mathrm{e}=\left[u_i^{(e)}(t),v_i^{(e)}(t),\ \emptyset_i^{(e)}(t),u_j^{(e)}(t),v_j^{(e)}(t),\ \emptyset_j^{(e)}(t)\ \right]^T \tag{16}$$

The displacement functions with nodal displacements are given as follows

$$u^{(\mathrm{e})}(X,\mathrm{t})=\left[\varphi^{(U)}\right]\begin{Bmatrix}u_\mathrm{i}\\u_\mathrm{j}\end{Bmatrix}=\left[\varphi^{(U)}\right]\{\mathrm{q}\}_U \tag{17a}$$

$$v^{(\mathrm{e})}(X,\mathrm{t})=\left[\varphi^{(V)}\right]\begin{Bmatrix}v_\mathrm{i}\\\emptyset_\mathrm{i}\\v_\mathrm{j}\\\emptyset_\mathrm{j}\end{Bmatrix}=\left[\varphi^{(V)}\right]\{q\}_V \tag{17b}$$

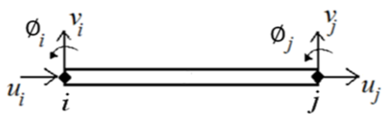

Fig. 2 Two-node finite element

$$\emptyset^{(\mathrm{e})}(X,\mathrm{t}) = \left[\varphi^{(\emptyset)}\right]\begin{Bmatrix} v_{\mathrm{i}} \\ \emptyset_{\mathrm{i}} \\ v_{\mathrm{j}} \\ \emptyset_{\mathrm{j}} \end{Bmatrix} = \left[\varphi^{(\emptyset)}\right]\{q\}_{\emptyset} \tag{17c}$$

where u_{i}, v_{i} and $\emptyset_{\mathrm{i}}$ are the node displacement components, $\varphi_i^{(U)}$, $\varphi_i^{(V)}$ and $\varphi_i^{(\emptyset)}$ indicate the shape functions. Interested reader can find the shape functions in Chakraborty *et al*. (2002). Substituting Eqs. (17a)-(17c) into energy Eqs. (8)-(14), the energy equations are obtained with shape functions and nodal displacements. Then, substituting the energy equations into equation (15), Lagrange's equations are obtained as follows

$$\frac{\partial I}{\partial q_k^{(e)}} - \frac{\partial}{\partial t}\frac{\partial I}{\partial \dot{q}_k^{(e)}} + Q_{D_k} = 0, \qquad Q_{D_k} = -\frac{\partial \mathrm{R}}{\partial \dot{q}_k^{(e)}}, \qquad k = 1,2,3,4,5,6 \tag{18}$$

where Q_{D_k} indicates generalized damping load. By using the Lagrange procedure, the equation of motion is given as follows

$$[K]\{q(t)\} + [D]\{\dot{q}(t)\} + [M]\{\ddot{q}(t)\} = \{F(t)\} \tag{19}$$

where $\{F\}$ is the load vector, $[K]$, $[D]$ and $[M]$ are element stiffness, damping and mass matrixes, respectively. Details of components of the finite element equation are given as follows

$$[K] = \begin{bmatrix} [K^U] & 0 & \left[K^{U\emptyset}\right] \\ 0 & [K^{\mathrm{V}}] & \left[K^{V\emptyset}\right] \\ \left[K^{\emptyset U}\right] & \left[K^{\emptyset V}\right] & \left[K^{\emptyset}\right] \end{bmatrix} \tag{20}$$

where

$$[K^U] = \int_0^{L_{\mathrm{e}}} A_{11}\left[\frac{\partial \varphi^{(U)}}{\partial X}\right]^T \left[\frac{\partial \varphi^{(U)}}{\partial X}\right] dX, \tag{21a}$$

$$\left[K^{U\emptyset}\right] = \left[K^{\emptyset U}\right]^{\mathrm{T}} = -\int_0^{L_{\mathrm{e}}} B_{11}\left[\frac{\partial \varphi^{(U)}}{\partial X}\right]^T \left[\frac{\partial \varphi^{(\emptyset)}}{\partial X}\right] dX, \tag{21b}$$

$$[K^V] = \int_0^{L_{\mathrm{e}}} \left(k_s A_{55}\left[\frac{\partial \varphi^{(V)}}{\partial X}\right]^T \left[\frac{\partial \varphi^{(V)}}{\partial X}\right] + \frac{1}{8}l^2 A_{55}\left[\frac{\partial^2 \varphi^{(V)}}{\partial X^2}\right]^T \left[\frac{\partial^2 \varphi^{(V)}}{\partial X^2}\right]\right) dX, \tag{21c}$$

$$\left[K^{V\emptyset}\right] = \left[K^{\emptyset V}\right]^{\mathrm{T}} = \int_0^{L_{\mathrm{e}}} \left(-k_s A_{55}\left[\frac{\partial \varphi^{(V)}}{\partial X}\right]^T \left[\varphi^{(\emptyset)}\right] + \frac{1}{8}l^2 A_{55}\left[\frac{\partial^2 \varphi^{(V)}}{\partial X^2}\right]^T \left[\frac{\partial \varphi^{(\emptyset)}}{\partial X}\right]\right) dX, \tag{21d}$$

$$\left[K^{\emptyset}\right] = \int_0^{L_{\mathrm{e}}} \left((D_{11} + \frac{1}{8}l^2 A_{55})\left[\frac{\partial \varphi^{(\emptyset)}}{\partial X}\right]^T \left[\frac{\partial \varphi^{(\emptyset)}}{\partial X}\right] + k_s A_{55}\left[\varphi^{(\emptyset)}\right]^T\left[\varphi^{(\emptyset)}\right]\right) dX, \tag{21e}$$

$$[M]=\begin{bmatrix}[M^U] & 0 & [M^{U\emptyset}]\\ 0 & [M^{\mathrm{V}}] & 0\\ [M^{U\emptyset}] & 0 & [M^{\emptyset}]\end{bmatrix} \tag{22}$$

where

$$[M_U]=\int_0^{L_\mathrm{e}} I_1\left[\varphi^{(U)}\right]^T\left[\varphi^{(U)}\right]dX \tag{23a}$$

$$[M_V]=\int_0^{L_\mathrm{e}} I_1\left[\varphi^{(V)}\right]^T\left[\varphi^{(V)}\right]dX \tag{23b}$$

$$[M_\theta]=\int_0^{L_\mathrm{e}} I_3\left[\varphi^{(\emptyset)}\right]^T\left[\varphi^{(\emptyset)}\right]dX \tag{23c}$$

$$[M_{U\theta}]=-\int_0^{L_\mathrm{e}} I_2\left[\varphi^{(\emptyset)}\right]^T\left[\varphi^{(U)}\right]dX \tag{23d}$$

$$[D]=\begin{bmatrix}[D^U] & 0 & [D^{U\emptyset}]\\ 0 & [D^{\mathrm{V}}] & [D^{V\emptyset}]\\ [D^{\emptyset U}] & [D^{\emptyset V}] & [D^{\emptyset}]\end{bmatrix} \tag{23}$$

where

$$[D^U]=\int_0^{L_\mathrm{e}} C_1\left[\frac{\partial\varphi^{(U)}}{\partial X}\right]^T\left[\frac{\partial\varphi^{(U)}}{\partial X}\right]dX \tag{25a}$$

$$\left[D^{U\emptyset}\right]=\left[D^{\emptyset U}\right]^{\mathrm{T}}=-\int_0^{L_\mathrm{e}} C_2\left[\frac{\partial\varphi^{(U)}}{\partial X}\right]^T\left[\frac{\partial\varphi^{(\emptyset)}}{\partial X}\right]dX \tag{25b}$$

$$[D^V]=\int_0^{L_\mathrm{e}}(k_sC_4\left[\frac{\partial\varphi^{(V)}}{\partial X}\right]^T\left[\frac{\partial\varphi^{(V)}}{\partial X}\right]+\frac{1}{8}l^2C_4\left[\frac{\partial^2\varphi^{(V)}}{\partial X^2}\right]^T\left[\frac{\partial^2\varphi^{(V)}}{\partial X^2}\right])dX \tag{25c}$$

$$\left[D^{V\emptyset}\right]=\left[K^{\emptyset V}\right]^{\mathrm{T}}=\int_0^{L_\mathrm{e}}\left(-k_sC_4\left[\frac{\partial\varphi^{(V)}}{\partial X}\right]^T\left[\varphi^{(\emptyset)}\right]+\frac{1}{8}l^2C_4\left[\frac{\partial^2\varphi^{(V)}}{\partial X^2}\right]^T\left[\frac{\partial\varphi^{(\emptyset)}}{\partial X}\right]\right)dX \tag{25d}$$

$$\left[D^{\emptyset}\right]=\int_0^{L_\mathrm{e}}((C_3+\tfrac{1}{8}l^2C_4)\left[\tfrac{\partial\varphi^{(\emptyset)}}{\partial X}\right]^T\left[\tfrac{\partial\varphi^{(\emptyset)}}{\partial X}\right]+k_sC_4\left[\varphi^{(\emptyset)}\right]^T\left[\varphi^{(\emptyset)}\right])\,)\mathrm{d} \tag{25e}$$

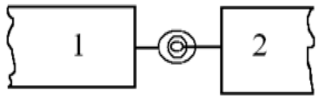

Fig. 3 Elastic rotational spring model in cracked microbeam

$$\{F(t)\} = \int_{x=0}^{L_e} \{\varphi(X)\}^T F(X,t)\ dX, \tag{26}$$

where L_e is the finite element length. In the crack model, an elastic rotational spring which connects the right and left sub-elements is used at the cracked cross-section, as shown Fig. 3.

According to elastic rotational spring model, compatibility conditions of the cracked location are

$$u_1 = u, \qquad v_1 = v_2, \qquad \Delta\emptyset = (\emptyset_1 - \emptyset_2) = k_M \frac{\partial^2 v}{\partial X^2} \qquad at \qquad X = L_1 \tag{27}$$

where k_M and $\Delta\emptyset$ are the flexibility constant and the slope increment respectively, at the cracked section. $\emptyset_1$ and $\emptyset_2$ indicate the angles on the two sides of the crack. Stiffness matrix, damping matrix and displacement vector of the cracked section for the spring model is given as follows

$$[K]_{(Cr)} = \begin{bmatrix} k_M & -k_M \\ -k_M & k_M \end{bmatrix}, \quad [D]_{(Cr)} = \eta_1 \begin{bmatrix} k_M & -k_M \\ -k_M & k_M \end{bmatrix}, \quad \{q\}_{(Cr)} = \{\emptyset_1,\ \emptyset_2\}^T \tag{28}$$

Substituting Eq. (28) into Eq. (19), the motion equation with crack is expressed as follows

$$\left([K] + [K]_{(Cr)}\right)\{q(t)\} + \left([D] + [D]_{(Cr)}\right)\{\dot{q}(t)\} + [M]\{\ddot{q}(t)\} = \{F(t)\} \tag{29}$$

In the solution of the motion equation (Eq. (29)), Newmark average acceleration method (Newmark 1959) is implemented in the time domain. The dimensionless quantities are expressed as

$$\eta = \frac{L_1}{L}, \quad K_T = \frac{K_M}{L} \tag{30}$$

where, η is the crack location ratio and K_T is the crack severity parameter.

3. Numerical results

Forced vibration responses of a cracked cantilever FGM microbeam are calculated and presented in figures in the MCST and the CBT for different the crack severity, material and geometry parameters. The material of the microbeam at middle surface (Y = 0) is chosen as Aluminum (E_0 = 70 GPa, ρ_0 = 2780 kg/m^3, v_0 = 0.33) and the material properties change exponentially according to Eq. (1). The length scale parameter taken as l = 15 μm (Akgöz and Civalek 2014). The finite element number is choosing as 100. In numerical process, five-point Gauss rule is used for calculation of the integration.). k_s is taken as 0.8922. The damping ratio η_1 is taken as $\eta_1 = 0.000001$ and η_2 and η_3 are taken as proportional to η_1 according to Eq.

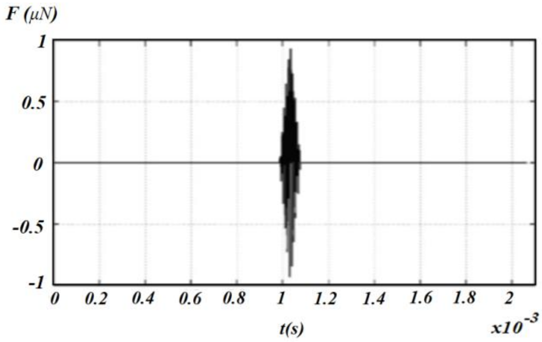

Fig. 4 The excitation of the force

Table 1 Validation study: the dimensionless frequencies for different values of $\boldsymbol{l}$ and $\boldsymbol{K_T}$

Frequency (*THz*)		$K_T = 0$	$K_T = 1$	$K_T = 2$
l = 10 μm	Tadi Beni *et al.* (2015)	0.02007	0.01651	0.01428
	Present study	0.02005	0.01648	0.01427
l = 20 μm	Tadi Beni *et al.* (2015)	0.04015	0.03303	0.02856
	Present study	0.04013	0.03300	0.02851
l = 30 μm	Tadi Beni *et al.* (2015)	0.06023	0.04953	0.04284
	Present study	0.06019	0.04949	0.04281

(7). For the forced vibration problem, a triangular impulse force ($F(t)$) e with a harmonic property at the free end is implemented as shown Fig. 4 in the time domain. The peak value of the impulse force is 1 μN.

In order to confirm the accuracy of presented method, a validation study is presented. In the validation study, the dimensionless fundamental frequencies with different values of l and K_T are obtained and compared with Tadi Beni *et al.* (2015) for $\eta = 0.5$ for MCST in Table 1. Material and geometry parameters used in Tadi Beni *et al.* (2015) are; epoxy, h = 300 nm, L= 1 μm, b = 100 nm. The results of present study agree with Tadi Beni *et al.* (2015)'s as shown Table 1.

In Fig. 5, the accelerations of the FGM microbeam are presented with different aspect ratios

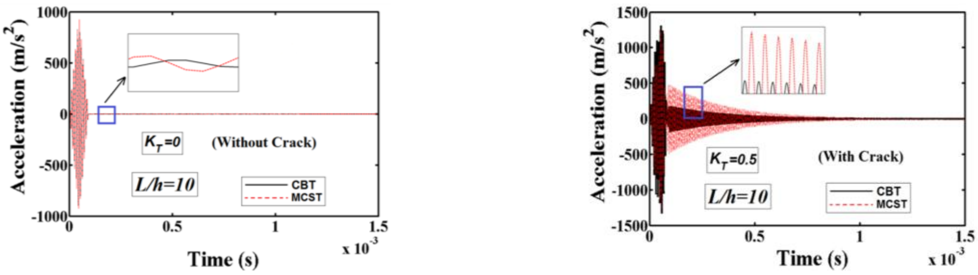

(a) For k_T = 0, L/h = 10 (b) For k_T = 0.5, L/h = 10

Fig. 5 The relationship between k_T and L/h on the accelerations of the FGM microbeam

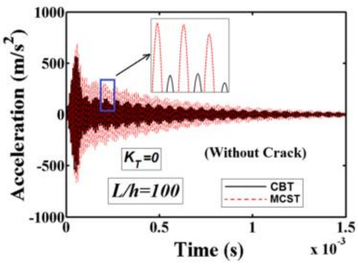

(c) For k_T = 0, L/h = 100

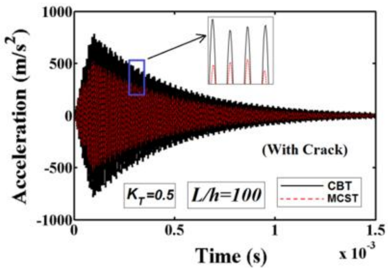

(d) For k_T = 0.5, L/h = 100

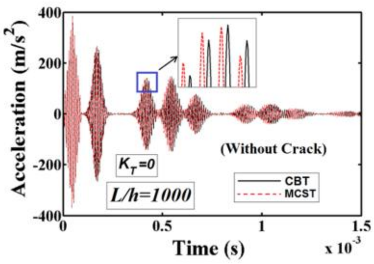

(e) For k_T = 0, L/h = 1000

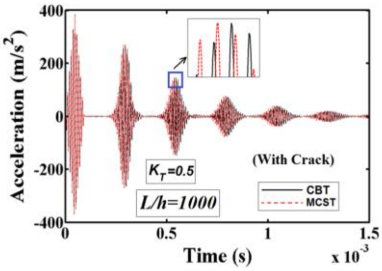

(f) For k_T = 0.5, L/h = 1000

Fig. 5 Continued

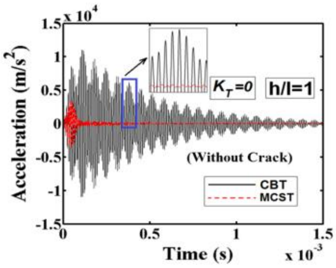

(a) For k_T = 0, h/l = 1

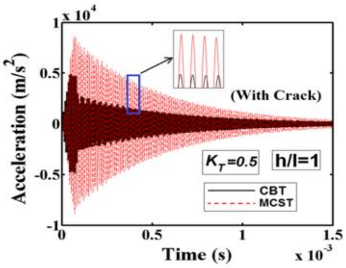

(b) For k_T = 0.5, h/l = 1

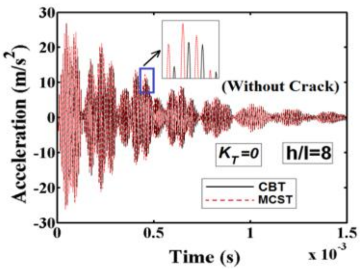

(c) For k_T = 0, h/l = 8

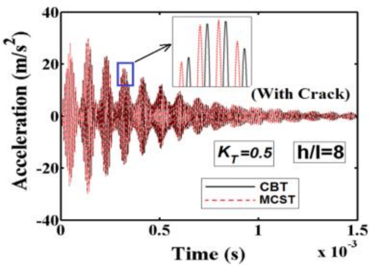

(d) For k_T = 0.5, h/l = 8

Fig. 6 The relationship between k_T and h/l on the accelerations of the FGM microbeam

(L/h) and the crack severity parameter for η = 0.5, h/l = 4 and $\beta = 0$ k_T in both MCST and CBT. It is noted that the accelerations are calculated at the free end. Fig. 5 shows that increase in the L/h, the difference between MCST and CBT diminishes. In high values of the L/h, the waves in both

CBT and MCST interfere with each other. Another result of Fig. 6 that the number of waves for both of CBT and MCST decrease as L/h increases. As seen from Fig. 5 that MCST must be used instead of CBT in the smaller value of aspect ratio. Increase in the L/h, the effect of the k_T, namely the crack effect, on the accelerations decrease. In higher L/h values, the effects of the k_T diminish significantly.

Fig. 6 displays the relationship between ratio of h/l and the accelerations for different the crack severity parameters k_T for $\eta = 0.5$, $\beta = 13000$ and for $L/h = 25$ in both CBT and MCST. It is noted that in the selection of the values of h/l, the height of the microbeam (h) is varied as l is keep constant as 15 μm. It is seen from Fig. 6 that the number of acceleration waves and the difference between the results of CBT and MCST decrease with increase in the D/l. Increase in the h/l, the effect of crack on the forced vibration responses decrease significantly. The accelerations in the CBT is larger than those of MCST without crack. However, the accelerations in the MCST is larger than those of CBT with crack. It shows that the crack is very effective for the forced vibration results of the microbeam and the difference between CBT and MCST.

In Fig. 7, the relationship between the material distribution parameter β and the accelerations

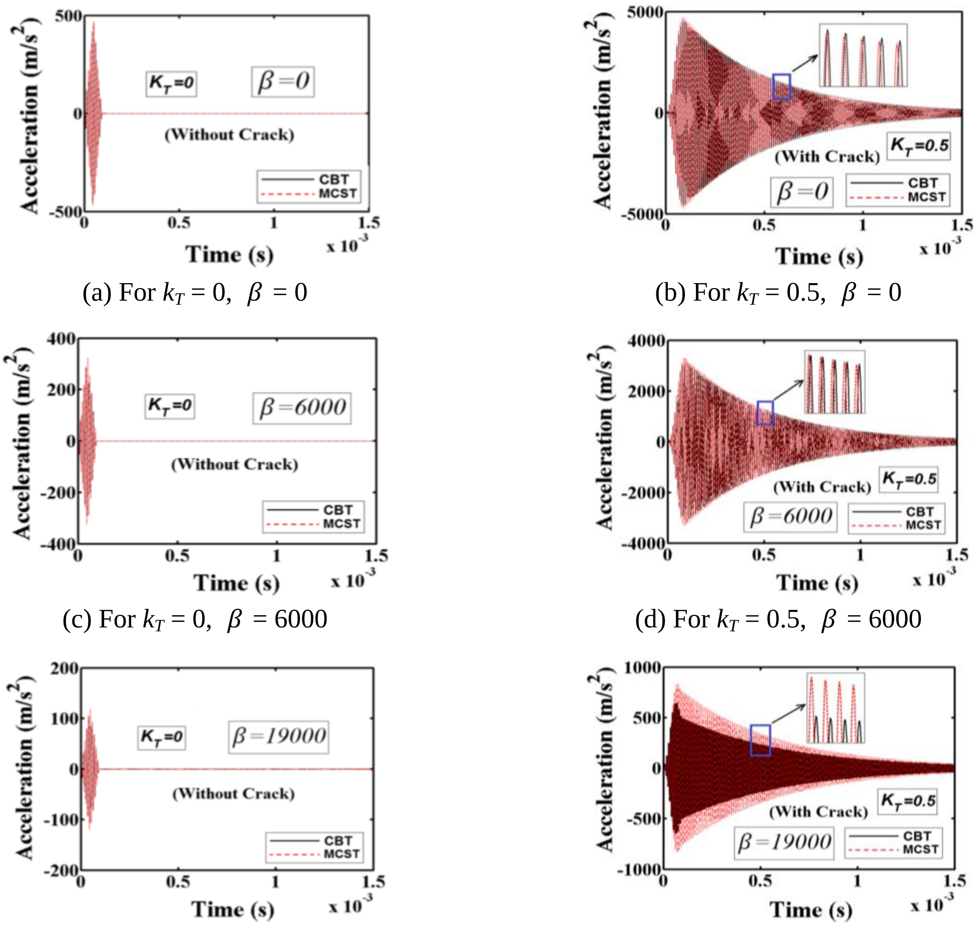

(a) For $k_T = 0$, $\beta = 0$ (b) For $k_T = 0.5$, $\beta = 0$

(c) For $k_T = 0$, $\beta = 6000$ (d) For $k_T = 0.5$, $\beta = 6000$

(e) For $k_T = 0$, $\beta = 19000$ (f) For $k_T = 0.5$, $\beta = 19000$

Fig. 7 The relationship between k_T and β on the accelerations of the FGM microbeam is plotted for different the crack severity parameters k_T for L/h = 10, h/l = 5 and η = 0.5 in both CBT and MCST. It is obvious from this figure that increasing the material distribution parameter β yields decreasing of the accelerations in both CBT and MCST. With increase in β, the Young's modulus and strength of FGM microbeam decrease according to Eq. (1). Hence, the strength of material decreases and accelerations increases naturally. Another result of Fig. 7 that increase in the material β, the difference between the CBT and MCST increases significantly. With decrease the β, the waves in both CBT and MCST interfere with each other. Increasing the β yields increasing of the number of waves. In addition, effects of the crack on the accelerations decrease considerably with increasing β. It shows that the material distribution parameter (β) is very effective to change in forced vibration responses of the cracked FGM microbeams.

4. Conclusions

Forced vibration of a cantilever FGM microbeam with crack and damping effects are studied for modified couple stress theory under a impulse force. In solution modeling of the problem, Timoshenko beam theory and finite element method are used within the Newmark method. Effects of crack, geometry and material properties on forced vibration results of the cracked microbeam are examined. The shortcomings of this study, the experimental investigation and accuracy are not included. It would be interesting to demonstrate the ability of the procedure through a wider campaign of investigations concerning experimental study of cracked micro/nano structures in the future. It is obtained from the result, the main conclusions are as follows:

- The L/h and h/l play determining role on the forced vibration of the cracked FGM microbeams.
- The crack parameters are very effective for the forced vibration results of the FGM microbeams and the difference between CBT and MCST.
- With increase in the L/h and h/l, number of acceleration waves and the difference between the CBT and MCST decrease considerably.
- In high values of the L/h and h/l, the acceleration waves of CBT and MCST interfere with each other.
- The crack parameters are very effective to change in the difference between the results of CBT and MCST.
- With decrease in the material distribution parameter β, the number waves and the difference between the CBT and MCST increase.
- The material distribution plays determining role in dynamic responses of the FGM microbeams.

References

Abdelaziz, H.H., Meziane, M.A.A., Bousahla, A.A., Tounsi, A., Mahmoud, S.R. and Alwabli, A.S. (2017), "An efficient hyperbolic shear deformation theory for bending, buckling and free vibration of FGM sandwich plates with various boundary conditions", *Steel Compos. Struct., Int. J.*, **25**(6), 693-704.

Ahouel, M., Houari, M.S.A., Bedia, E.A. and Tounsi, A. (2016), "Size-dependent mechanical behavior of functionally graded trigonometric shear deformable nanobeams including neutral surface position concept", *Steel Compos. Struct., Int. J.*, **20**(5), 963-981.

Aissani, K., Bouiadjra, M.B., Ahouel, M. and Tounsi, A. (2015), "A new nonlocal hyperbolic shear deformation theory for nanobeams embedded in an elastic medium", *Struct. Eng. Mech., Int. J.*, **55**(4), 743-763.

Akbaş, Ş.D. (2013), "Geometrically nonlinear static analysis of edge cracked Timoshenko beams composed of functionally graded material", *Math. Problems Eng.*

Akbaş, Ş.D. (2015a), "On Post-Buckling Behavior of Edge Cracked Functionally Graded Beams Under Axial Loads", *Int. J. Struct. Stabil. Dyn.*, **15**(4), 1450065. DOI: 10.1142/S0219455414500655

Akbaş, Ş.D. (2015b), "Post-Buckling Analysis of Axially Functionally Graded Three Dimensional Beams", *Int. J. Appl. Mech.*, **7**(3),1550047. DOI: 10.1142/S1758825115500477

Akbaş, Ş.D. (2016a), "Forced vibration analysis of viscoelastic nanobeams embedded in an elastic medium", *Smart Struct. Syst., Int. J.*, **18**(6), 1125-1143.

Akbaş, Ş.D. (2016b), "Analytical solutions for static bending of edge cracked micro beams", *Struct. Eng. Mech., Int. J.*, **59**(3), 579-599.

Akbaş, Ş.D. (2017a), "Free vibration of edge cracked functionally graded microscale beams based on the modified couple stress theory", *Int. J. Struct. Stabil. Dyn.*, **17**(3), 1750033.

Akbaş Ş.D. (2017b), "Static, Vibration, and Buckling Analysis of Nanobeams", In: *Nanomechanics*, (A. Vakhrushev Ed.), InTech, pp.123-137.

Akbaş, Ş.D. (2017c), "Stability of A Non-Homogenous Porous Plate by Using Generalized Differantial Quadrature Method", *Int. J. Eng. Appl. Sci.*, **9**(2), 147-155.

Akbaş, Ş.D. (2017d), "Forced vibration analysis of functionally graded nanobeams", *Int. J. Appl. Mech.*, **9**(7), 1750100.

Akbas, S.D. (2017e), "Post-buckling responses of functionally graded beams with porosities", *Steel Compos. Struct., Int. J.*, **24**(5), 579-589.

Akbaş, Ş.D. (2017f), "Vibration and static analysis of functionally graded porous plates", *J. Appl. Computat. Mech.*, **3**(3), 199-207.

Akbaş, Ş.D. (2018), "Forced vibration analysis of functionally graded porous deep beams", *Compos. Struct.*, **186**, 293-302.

Akbaş, Ş.D. and Kocatürk, T. (2013), "Post-buckling analysis of functionally graded three-dimensional beams under the influence of temperature", *J. Therm. Stresses*, **36**(12), 1233-1254.

Akgöz, B. and Civalek, Ö. (2013), "Free vibration analysis of axially functionally graded tapered Bernoulli-Euler microbeams based on the modified couple stress theory", *Compos. Struct.*, **98**, 314-322.

Akgöz, B. and Civalek, Ö. (2014), "Thermo-mechanical buckling behavior of functionally graded microbeams embedded in elastic medium", *Int. J. Eng. Sci.*, **85**, 90-104.

Al-Basyouni, K.S., Tounsi, A. and Mahmoud, S.R. (2015), "Size dependent bending and vibration analysis of functionally graded micro beams based on modified couple stress theory and neutral surface position", *Compos. Struct.*, **125**, 621-630.

Ansari, R., Gholami, R. and Sahmani, S. (2011), "Free vibration analysis of size-dependent functionally graded microbeams based on the strain gradient Timoshenko beam theory", *Compos. Struct.*, **94**(1), 221-228.

Ansari, R., Gholami, R. and Sahmani, S. (2014), "Free vibration of size-dependent functionally graded microbeams based on the strain gradient Reddy beam theory", *Int. J. Computat. Methods Eng. Sci. Mech.*, **15**(5), 401-412.

Asghari, M., Ahmadian, M.T., Kahrobaiyan, M.H. and Rahaeifard, M. (2010), "On the size-dependent behavior of functionally graded micro-beams", *Mater. Des.*, **31**(5), 2324-2329.

Attia, M.A. (2017), "On the mechanics of functionally graded nanobeams with the account of surface elasticity", *Int. J. Eng. Sci.*, **115**, 73-101.

Belabed, Z., Houari, M.S.A., Tounsi, A., Mahmoud, S.R. and Anwar Bég, O. (2014), "An efficient and simple higher order shear and normal deformation theory for functionally graded material (FGM) plates", *Compos.*; *Part B*, **60**, 274-283.

Belkorissat, I., Houari, M.S.A., Tounsi, A., Bedia, E.A. and Mahmoud, S.R. (2015), "On vibration properties of functionally graded nano-plate using a new nonlocal refined four variable model", *Steel*

Compos. *Struct*., *Int*. *J*., **18**(4), 1063-1081.

Bellifa, H., Benrahou, K.H., Bousahla, A.A., Tounsi, A. and Mahmoud, S.R. (2017), "A nonlocal zeroth-order shear deformation theory for nonlinear postbuckling of nanobeams", *Struct*. *Eng*. *Mech*., *Int*. *J*., **62**(6), 695-702.

Bennoun, M., Houari, M.S.A. and Tounsi, A. (2016), "A novel five-variable refined plate theory for vibration analysis of functionally graded sandwich plates", *Mech*. *Adv*. *Mater*. *Struct*., **23**(4), 423-431.

Besseghier, A., Houari, M.S.A., Tounsi, A. and Mahmoud, S.R. (2017), "Free vibration analysis of embedded nanosize FG plates using a new nonlocal trigonometric shear deformation theory", *Smart Struct*. *Syst*., *Int*. *J*., **19**(6), 601-614.

Bouafia, K., Kaci, A., Houari, M.S.A., Benzair, A. and Tounsi, A. (2017), "A nonlocal quasi-3D theory for bending and free flexural vibration behaviors of functionally graded nanobeams", *Smart Struct*. *Syst*., *Int*. *J*., **19**(2), 115-126.

Boukhari, A., Atmane, H.A., Tounsi, A., Adda, B. and Mahmoud, S.R. (2016), "An efficient shear deformation theory for wave propagation of functionally graded material plates", *Struct*. *Eng*. *Mech*., *Int*. *J*., **57**(5), 837-859.

Bourada, M., Kaci, A., Houari, M.S.A. and Tounsi, A. (2015), "A new simple shear and normal deformations theory for functionally graded beams", *Steel Compos*. *Struct*., *Int*. *J*., **18**(2), 409-423.

Bounouara, F., Benrahou, K.H., Belkorissat, I. and Tounsi, A. (2016), "A nonlocal zeroth-order shear deformation theory for free vibration of functionally graded nanoscale plates resting on elastic foundation", *Steel Compos*. *Struct*., *Int*. *J*., **20**(2), 227-249.

Bousahla, A.A., Houari, M.S.A., Tounsi, A. and Adda Bedia, E.A. (2014), "A novel higher order shear and normal deformation theory based on neutral surface position for bending analysis of advanced composite plates", *Int*. *J*. *Computat*. *Methods*, **11**(6), 1350082.

Chaht, F.L., Kaci, A., Houari, M.S.A., Tounsi, A., Bég, O.A. and Mahmoud, S.R. (2015), "Bending and buckling analyses of functionally graded material (FGM) size-dependent nanoscale beams including the thickness stretching effect", *Steel Compos*. *Struct*., *Int*. *J*., **18**(2), 425-442.

Chorsi, M.T., Azizi, S. and Bakhtiari-Nejad, F. (2017), "Nonlinear dynamics of a functionally graded piezoelectric micro-resonator in the vicinity of the primary resonance", *J*. *Vib*. *Control*, **23**(3), 400-413.

Chakraborty, A., Mahapatra, D.R. and Gopalakrishnan, S. (2002), "Finite element analysis of free vibration and wave propagation in asymmetric composite beams with structural discontinuities", *Compos*. *Struct*., **55**(1), 23-36.

Demir, Ç. and Civalek, Ö. (2017), "On the analysis of microbeams", *Int*. *J*. *Eng*. *Sci*., **121**, 14-33.

Ebrahimi, F. and Barati, M.R. (2016a), "Vibration analysis of smart piezoelectrically actuated nanobeams subjected to magneto-electrical field in thermal environment", *J*. *Vib*. *Control*, 1077546316646239.

Ebrahimi, F. and Salari, E. (2015), "Size-dependent thermo-electrical buckling analysis of functionally graded piezoelectric nanobeams", *Smart Mater*. *Struct*., **24**(12), 125007.

Ebrahimi, F. and Shafiei, N. (2016b), "Application of Eringen's nonlocal elasticity theory for vibration analysis of rotating functionally graded nanobeams", *Smart Struct*. *Syst*., *Int*. *J*., **17**(5), 837-857.

Ebrahimi, F., Barati, M.R. and Haghi, P. (2017), "Wave propagation analysis of size-dependent rotating inhomogeneous nanobeams based on nonlocal elasticity theory", *J*. *Vib*. *Control*, 1077546317711537.

Eringen, A.C. (1972), "Nonlocal polar elastic continua", *Int*. *J*. *Eng*. *Sci*., **10**(1), 1-16.

Fang, T.H., Chang, W.J. and Liao, S.C. (2003), "Simulated nanojet ejection process by spreading droplets on a solid surface", *J*. *Phys*.; *Condensed Matter*, **15**(49), 8263-8271.

Fang, T.H. and Chang, W.J. (2003), "Sensitivity analysis of scanning near-field optical microscope probe", *Optics Laser Technol*., **35**(4), 267-271.

Fu, Y., Du, H. and Zhang, S. (2003), "Functionally graded TiN/TiNi shape memory alloy films", *Mater*. *Lett*., **57**(20), 2995-2999.

Hadji, L. (2017), "Analysis of functionally graded plates using a sinusoidal shear deformation theory", *Smart Struct*. *Syst*., *Int*. *J*., **19**(4), 441-448.

Hadji, L., Khelifa, Z. and Adda Bedia, E.A. (2016), "A New Higher Order Shear Deformation Model for Functionally Graded Beams", *KSCE J*. *Civil Eng*., **20**(5), 1835-1841.

Hamidi, A., Houari, M.S.A., Mahmoud, S.R. and Tounsi, A. (2015), "A sinusoidal plate theory with 5-unknowns and stretching effect for thermomechanical bending of functionally graded sandwich plates", *Steel Compos. Struct., Int. J.*, **18**(1), 235-253.

Hasanyan, D.J., Batra, R.C. and Harutyunyan, S. (2008), "Pull-in instabilities in functionally graded microthermoelectromechanical systems", *J. Therm. Stresses*, **31**(10), 1006-1021.

Hasheminejad, B.S.M., Gheshlaghi, B., Mirzaei, Y. and Abbasion, S. (2011), "Free transverse vibrations of cracked nanobeams with surface effects", *Thin Solid Films*, **519**(8), 2477-2482.

Hebali, H., Tounsi, A., Houari, M.S.A., Bessaim, A. and Bedia, E.A.A. (2014), "New quasi-3D hyperbolic shear deformation theory for the static and free vibration analysis of functionally graded plates", *J. Eng. Mech.*, **140**(2), 374-383.

Houari, M.S.A., Tounsi, A., Bessaim, A. and Mahmoud, S.R. (2016), "A new simple three-unknown sinusoidal shear deformation theory for functionally graded plates", *Steel Compos. Struct., Int. J.*, **22**(2), 257-276.

Karami, B., Janghorban, M. and Tounsi, A. (2017), "Effects of triaxial magnetic field on the anisotropic nanoplates", *Steel Compos. Struct., Int. J.*, **25**(3), 361-374.

Ke, L.L., Wang, Y.S., Yang, J. and Kitipornchai, S. (2012), "Nonlinear free vibration of size-dependent functionally graded microbeams", *Int. J. Eng. Sci.*, **50**(1), 256-267.

Khetir, H., Bouiadjra, M.B., Houari, M.S.A., Tounsi, A. and Mahmoud, S.R. (2017), "A new nonlocal trigonometric shear deformation theory for thermal buckling analysis of embedded nanosize FG plates", *Struct. Eng. Mech., Int. J.*, **64**(4), 391-402.

Kocatürk, T. and Akbaş, Ş.D. (2013a), "Thermal post-buckling analysis of functionally graded beams with temperature-dependent physical properties", *Steel Compos. Struct., Int. J.*, **15**(5), 481-505.

Kocatürk, T. and Akbaş, Ş.D. (2013b), "Wave propagation in a microbeam based on the modified couple stress theory", *Struct. Eng. Mech., Int. J.*, **46**(3), 417-431.

Lam, D.C.C., Yang, F., Chong, A.C.M., Wang, J. and Tong, P. (2003), "Experiments and theory in strain gradient elasticity", *J. Mech. Phys. Solids*, **51**(8), 1477-1508.

Liu, P. and Reddy, J.N. (2011), "A Nonlocal curved beam model based on a modified couple stress theory", *Int. J. Struct. Stabil. Dyn.*, **11**(3), 495-512.

Liu, S.J., Qi, S.H. and Zhang, W.M. (2013), "Vibration behavior of a cracked micro-cantilever beam under electrostatic excitation", *Zhendong yu Chongji/J. Vib. Shock*, **32**, 41-45.

Loya, J., López-Puente, J., Zaera, R. and Fernández-Sáez, J. (2009), "Free transverse vibrations of cracked nanobeams using a nonlocal elasticity model", *J. Appl. Phys.*, **105**(4), 044309.

Lü, C.F., Lim, C.W. and Chen, W.Q. (2009), "Size-dependent elastic behavior of FGM ultra-thin films based on generalized refined theory", *Int. J. Solids Struct.*, **46**(5), 1176-1185.

Mahi, A., Adda Bedia, E.A. and Tounsi, A. (2015), "A new hyperbolic shear deformation theory for bending and free vibration analysis of isotropic, functionally graded, sandwich and laminated composite plates", *Appl. Math. Model.*, **39**(9), 2489-2508.

Meziane, M.A.A., Abdelaziz, H.H. and Tounsi, A. (2014), "An efficient and simple refined theory for buckling and free vibration of exponentially graded sandwich plates under various boundary conditions", *J. Sandw. Struct. Mater.*, **16**(3), 293-318.

Mindlin, R.D. and Tiersten, H.F. (1962), "Effects of couple-stresses in linear elasticity", *Arch. Rational Mech. Anal.*, **11**(1), 415-448.

Mindlin, R.D. (1963), "Influence of couple-stresses on stress concentrations", *Experim. Mech.*, **3**(1), 1-7.

Mouffoki, A., Adda Bedia, E.A., Houari, M.S.A., Tounsi, A. and Mahmoud, S.R. (2017), "Vibration analysis of nonlocal advanced nanobeams in hygro-thermal environment using a new two-unknown trigonometric shear deformation beam theory", *Smart Struct. Syst., Int. J.*, **20**(3), 369-383.

Nejad, M.Z. and Hadi, A. (2016a), "Eringen's non-local elasticity theory for bending analysis of bi-directional functionally graded Euler–Bernoulli nano-beams", *Int. J. Eng. Sci.*, **106**, 1-9.

Nejad, M.Z. and Hadi, A. (2016b), "Non-local analysis of free vibration of bi-directional functionally graded Euler–Bernoulli nano-beams", *Int. J. Eng. Sci.*, **105**, 1-11.

Newmark, N.M. (1959), "A method of computation for structural dynamics", *ASCE Eng. Mech. Div.*, **85**(3),

67-94.
Park, S.K. and Gao, X.L. (2006), “Bernoulli–Euler beam model based on a modified couple stress theory”, *J. Micromech. Microeng.*, **16**(11), 2355-2359.
Peng, X.-L., Li. X.-F., Tang, G.-J. and Shen, Z.-B. (2015), “Effect of scale parameter on the deflection of a nonlocal beam and application to energy release rate of a crack”, *ZAMM – J. Appl. Math. Mech.*, **95**(12), 1428-1438.
Roostai, H. and Haghpanahi, M. (2014), “Vibration of nanobeams of different boundary conditions with multiple cracks based on nonlocal elasticity theory”, *Appl. Math. Model.*, **38**(3), 1159-1169.
Salamat-Talab, M., Nateghi, A. and Torabi, J. (2012), “Static and dynamic analysis of third-order shear deformation FG micro beam based on modified couple stress theory”, *Int. J. Mech. Sci.*, **57**(1), 63-73.
Sedighi, H.M. (2014), “The influence of small scale on the pull-in behavior of nonlocal nanobridges considering surface effect, Casimir and Van der Waals attractions”, *Int. J. Appl. Mech.*, **6**(3), 1450030.
Sedighi, H.M., Koochi, A. and Abadyan, M. (2014), “Modeling the size dependent static and dynamic pull-in instability of cantilever nanoactuator based on strain gradient theory”, *Int. J. Appl. Mech.*, **6**(5), 1450055.
Shafiei, N., Mousavi, A. and Ghadiri, M. (2016), “On size-dependent nonlinear vibration of porous and imperfect functionally graded tapered microbeams”, *Int. J. Eng. Sci.*, **106**, 42-56.
Stamenković, M., Karličić, D., Goran, J. and Kozić, P. (2016), “Nonlocal forced vibration of a double single-walled carbon nanotube system under the influence of an axial magnetic field”, *J. Mech. Mater. Struct.*, **11**(3), 279-307.
Şimşek, M. and Reddy, J.N. (2013), “Bending and vibration of functionally graded microbeams using a new higher order beam theory and the modified couple stress theory”, *Int. J. Eng. Sci.*, **64**, 37-53.
Şimşek, M., Kocatürk, T. and Akbaş, Ş.D. (2013), “Static bending of a functionally graded microscale Timoshenko beam based on the modified couple stress theory”, *Compos. Struct.*, **95**, 740-747.
Tadi Beni, Y., Jafari, A. and Razavi, H. (2015), “Size effect on free transverse vibration of cracked nano-beams using couple stress theory”, *Int. J. Eng.*, **28**(2), 296-304
Tagrara, S.H., Benachour, A., Bouiadjra, M.B. and Tounsi, A. (2015), “On bending, buckling and vibration responses of functionally graded carbon nanotube-reinforced composite beams”, *Steel Compos. Struct., Int. J.*, **19**(5), 1259-1277.
Torabi, K. and Nafar Dastgerdi, J. (2012), “An analytical method for free vibration analysis of Timoshenko beam theory applied to cracked nanobeams using a nonlocal elasticity model”, *Thin Solid Films*, **520**(21), 6595-6602.
Toupin, R.A. (1962), “Elastic materials with couple stresses”, *Arch. Rational Mech. Anal.*, **11**(1), 385-414.
Wang, C.M., Xiang, Y., Yang, J. and Kitipornchai, S. (2012), “Buckling of nano-rings/arches based on nonlocal elasticity”, *Int. J. Appl. Mech.*, **4**(3), 1250025.
Wang, K. and Wang, B. (2015), “Timoshenko beam model for the vibration analysis of a cracked nanobeam with surface energy”, *J. Vib. Control*. DOI: 10.1177/1077546313513054
Witvrouw, A. and Mehta, A. (2005), “The use of functionally graded Poly-SiGe Layers for MEMS Applications”, *Mater. Sci. Forum*, **492**, 255-260.
Yahia, S.A., Atmane, H.A., Houari, M.S.A. and Tounsi, A. (2015), “Wave propagation in functionally graded plates with porosities using various higher-order shear deformation plate theories”, *Struct. Eng. Mech., Int. J.*, **53**(6), 1143-1165.
Yang, F., Chong, A., Lam, D. and Tong, P. (2002), “Couple stress based strain gradient theory for elasticity”, *Int. J. Solids Struct.*, **39**(10), 2731-2743.
Yaylı, M.O. and Çerçevik, A.E. (2015), “Axial vibration analysis of cracked nanorods with arbitrary boundary conditions”, *J. Vibroeng.*, **17**(6), 2907-2921.
Zamanzadeh, M., Rezazadeh, G., Jafarsadeghi-Pournaki, I. and Shabani, R. (2014), “Thermally induced vibration of a functionally graded micro-beam subjected to a moving laser beam”, *Int. J. Appl. Mech.*, **6**(6), 1450066.
Zhang, J. and Fu, Y. (2012), “Pull-in analysis of electrically actuated viscoelastic microbeams based on a modified couple stress theory”, *Meccanica*, **47**(7), 1649-1658.

Zouatnia, N., Hadji, L. and Kassoul, A. (2017), "An analytical solution for bending and vibration responses of functionally graded beams with porosities", *Wind Struct*., *Int*. *J*., **25**(4), 329-342.

CC